

# Binarized ResNet: Enabling Automatic Modulation Classification at the resource-constrained Edge

Nitin Priyadarshini Shankar, Deepsayan Sadhukhan, Nancy Nayak, and Sheetal Kalyani

**Abstract**—In this paper, we propose a ResNet based neural architecture to solve the problem of Automatic Modulation Classification. We showed that our architecture outperforms the state-of-the-art (SOTA) architectures. We further propose to binarize the network to deploy it in the Edge network where the devices are resource-constrained i.e. have limited memory and computing power. Instead of simple binarization, rotated binarization is applied to the network which helps to close the significant performance gap between the real and the binarized network. Because of the immense representation capability of the real network, its rotated binarized version achieves 85.33% accuracy compared to 95.76% accuracy of the proposed real network with 2.33 and 16 times lesser computing power than two of the SOTA architectures, MCNet and RMLResNet respectively, and approximately 16 times less memory than both. The performance can be improved further to 87.74% by taking an ensemble of four such rotated binarized networks.

**Index Terms**—Deep Learning, Wireless communication, Automatic Modulation Classification, Binary Neural Network, Ensemble Bagging, Computation and memory efficiency.

## I. INTRODUCTION

Automatic Modulation Classification (AMC) has a wide variety of applications in wireless communication ranging from military applications to civil and commercial use [1]–[5]. At the receiver, before any signal processing, the classification of the modulation type of the transmitted signal in real-time is necessary to avoid control overhead. The likelihood-based (LB) AMC methods [6]–[8] are computationally complex even though they can achieve optimal solutions theoretically. On the other hand, the feature-based (FB) methods which have two parts namely (i) feature extractor (FE) and (ii) classifier reach a sub-optimal solution with very low complexity and hence, are of significant interest. The performance of traditional FB methods primarily depends on different features that are manually extracted; such as instantaneous statistics, high-order statistics, time-frequency characteristics, the probability density function of signal phase, etc. [9]–[12]. The features are then compared with a threshold or fed to a pattern recognizer. Sometimes the manual selection of features may not be able to differentiate the characteristics of a signal from one modulation to another. To extract the best combination of features automatically while adapting to the set of modulations and different channel environments, feature extractors based on several deep learning models like Convolutional Neural Network (CNN) [13]–[16], GoogLeNet [17], Deep Belief Network [18], Recurrent Neural

Network-based Long Short Term Memory (LSTM) [19], and ResNet [20] have gained immense popularity. In [21], the authors proposed to use contrast-enhanced grid constellation images along with regular constellation images as input to capture high dimensional features. As the FB methods give sub-optimal solutions occasionally, there has been an increased focus on improving the classification accuracy by advancing the feature extractor, thus leading to the use of more complex neural networks. However, because of a large number of network parameters, the models generally overfit leading to limited classification accuracy [20]. In this paper, inspired by the image classification problem [22], we propose a ResNet based architecture called *LResNet18A* for AMC trained using RML2018.01a dataset that has 24 modulation classes. The proposed FE architecture is based on 2D convolutional filters that extract the features omnidirectionally and therefore the architecture does not overfit.

Note that the deployment of such a complex FE is challenging to the receiver where high computing power is not available. So, for green communication, the AMC model deployed at the resource-constrained devices should consume less memory and be computationally efficient, yet have competent accuracy. Recently there is an increased interest in FEs that are computationally less demanding to achieve lower latency without any degradation in performance. In [23] a fast and robust method for AMC using Kolmogorov-Smirnov Test was proposed. A bottleneck and asymmetric convolution structure are employed in [24] to reduce computational complexity. In [15], a grid constellation-based AMC method based on contrastive fully Convolutional NN (CFCN) was proposed that enlarges the discrepancies among different modulations and reduce training time. For the same purpose, a recently proposed ResNet-based AMC using involution named (InvResNet) was proposed in [25] that achieves better accuracy than RMLResNet [20] (one of the SOTA architectures) and has a faster convergence. In [26], the authors proposed distributed learning-based AMC that relies on the cooperation of multiple edge devices. The real-valued networks take up a lot of memory and consume a lot of power due to high complexity and computation cost.

With the rising number of mobile devices at the edge network that consumes low power, has lower memory capacity, and computation power, we need economic battery usage to extend battery life. Because of the massive number of such devices, there is an excessive signal processing requirement at the user end that increases the power consumption. For such edge devices, we propose compact architectures called Binarized LResNet18A (*BLResNet18A*) using Binary Neural

The authors are with the Department of Electrical Engineering, Indian Institute of Technology Madras, India.

Emails:

{ee20d425@smail, ee20s001@smail, ee17d408@smail, skalyani@ee}.iitm.ac.in

Networks (BNNs) [27] where we binarize the filters, weights, biases, and activations. Different variants of BNNs [28]–[30] are proposed for use for traditional ML applications not only to avoid generalization error but also to achieve faster computation during deployment with one-bit xnor and bitcount operations [31]. But if the real network does not have enough complexity to extract the features, the regular BNN version suffers from poor representation power and has lower accuracy. At present, there is very little literature on BNNs for wireless communication applications. The use of BNN to produce the Turbo code in a wireless edge network was proposed in [27] to reduce the memory requirement and computation 64 times; further, an ensemble of  $K$  such BNNs closes the performance gap between the binary and the real version with  $K$  times increase in the memory. However, blindly binarizing any full-precision DL network for any application degrades the performance. For example, [32] and [19] highlight that binarization of LSTM and CNNs lead to severe degradation in performance.

Recently a Rotated BNN was proposed in machine learning literature [33] to improve the accuracy of BNN. By implementing RBNN, the angular bias between the real-valued parameters and its binary version is reduced during training leading to around 50% weight flips which maximizes the information gain. In this work, we show that the RBNN version of any arbitrary architecture does not perform equal to its real counterpart. The Architecture has to be chosen carefully so that the rotated binarized version has enough representation power to learn the application at hand. Further, we propose *RBLResNet18A*, the RBNN version of the proposed LResNet18A is shown to have a performance very close to all the real networks, reduced memory complexity by a factor of 64, and is 64 times faster in computation. Hence, we can save on memory and computation without compromising the accuracy of the classification. To study our architectures, we have taken MCNet [34] and RMLResNet [20] architectures for comparison (more details in next section). In summary,

- We propose LResNet18A architecture for AMC and show that it has a performance equivalent to InvoResNet [25] but with a much lower computation at the cost of more memory.
- We then propose RBLResNet18A, the RBNN version of the proposed architecture that has reduced memory and computing power.
- The performance is improved further by taking an ensemble of the RBLResNet18A architectures.
- We provide an extensive comparison with two different methods, RMLResNet and MCNet, and show that the proposed RBLResNet18A has approximately 16 times lesser memory and 2.33 times lesser complex than MCNet and is 16 times lesser complex than RMLResNet. Codes for all the experiments are available at <https://github.com/deepsy1998/RBLResNet>.

## II. DL BASED POPULAR AMC METHODS

Recently some state-of-the-art models have been tested on the *RML2018.01a* dataset having 24 modulation classes.

Having such a large number of classes makes it a challenging problem in the field of modulation recognition. In the ResNet-based method for AMC, referred to as *RMLResNet* [20], the authors approached the modulation recognition problem with a modified residual network, a first of its kind that obtained improved performance over other CNN methods. However, this model has a higher convergence time. Later several works tried to achieve better accuracy by improving the architecture. For example, the authors in *MCNet* [34] proposed an architecture that has several specific convolutional blocks to concurrently learn the Spatio-temporal correlations using asymmetric convolutional kernels. The blocks also have skip connections like [20] to address the problem of vanishing gradient and have asymmetric kernel sizes. For such a system, accuracy improves only at the cost of additional blocks elevating memory and complexity. In *InvoResNet* [25] the authors proposed a novel involution method over convolution to enhance discrimination capability and expressiveness of the model. Even though it is said to have faster convergence, it has huge computational complexity as shown in Table. II, Sec. IV. In *LightWeight* [35], a model similar to MCNet [34] is used. The model has asymmetric kernel dimensions ( $1 \times 3$  and  $3 \times 1$ ) to reduce the number of parameters and considers only a part of the dataset to reduce complexity but, such a model has poor representation power on binarizing due to less number of parameters and MCNet with 10 blocks outperforms them.

## III. PROPOSED ARCHITECTURE

In this context, we propose a Residual network architecture LResNet18A having a higher number of output filters with increasing depth that increases the number of parameters leading to higher representation power. The core of the proposed architecture contains Residual units whose couple is called a ResNet block. The main advantage of a ResNet block is the presence of skipped connections which adds the input to a later stage of the block enabling the network to learn the Residual. It helps the network to overcome the vanishing gradients problem.

Each ResNet block has convolutional layers as its fundamental entity as shown in Fig. 1. The architecture mainly has two different types of Residual blocks as illustrated in Fig. 1b and Fig. 1c according to whether we need to reduce the spatial dimension or not. The only difference between the two blocks is the addition of a convolution layer with  $1 \times 1$  kernel size to reduce the spatial dimension whenever required.

The proposed architecture contains symmetric 2D filters of dimension ( $3 \times 3$ ) that can extract the features omnidirectionally (diagonal compared to existing horizontal and vertical feature extraction). The number of filters are gradually increased from 32 to 128 in a span of 4 such blocks extracting the finer details as we go in-depth. The first convolutional layer is designed to extract general features without altering the spatial dimension of the input and has 32 filters of shape  $3 \times 3$ . Then we perform a 2D Batch Normalisation along the spatial dimensions of the output of the convolutional layer. It is practiced for all the convolutional layers since it increases the stability and reduces the number of epochs required for training.

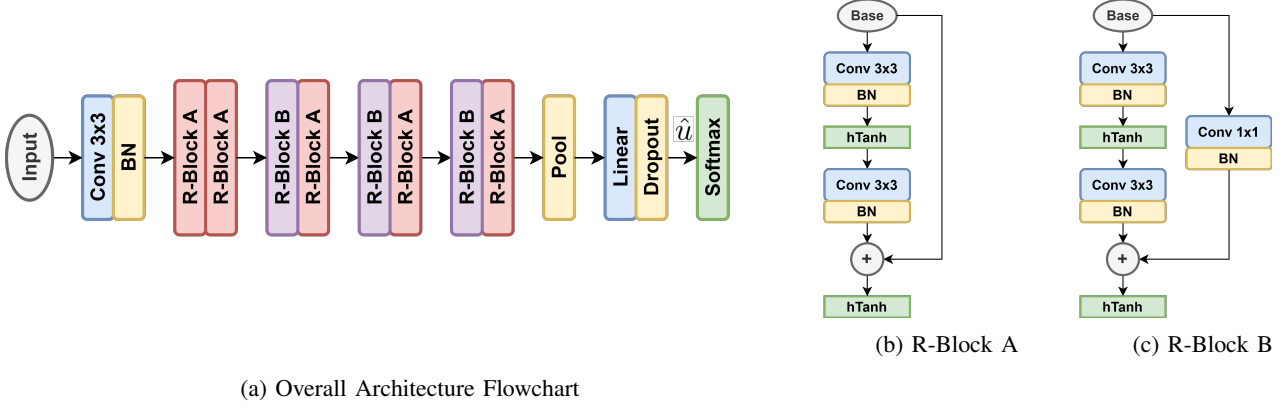


Fig. 1: Proposed architecture and two types of ResNet blocks: R-Block A and R-Block B

The *hard tanh* activation function is used in all the blocks except at the output where a softmax activation is used. After stacking several of these blocks together, we perform an average-pooling operation followed by a 2D Batch Normalisation, a linear layer (with softmax activation) to perform classification. A dropout layer is included to prevent overfitting. The details of the architecture are provided in Table. I.

We were inspired to build the proposed architecture based on the image classification problem of the CIFAR-10 dataset [22] as the number of input features of a single sample ( $32 \times 32 = 1024$ ) in the CIFAR-10 dataset is of the same order as that of the number of input features in the RML2018.01a dataset ( $2 \times 1024 = 2048$ ). Though the proposed architecture has better or equivalent performance when compared with InvoResNet (the current state of the art in terms of performance), it is nearly 2090 times less computationally complex. However, it requires about 3 times of memory of InvoResNet. Given the current focus of green communication and low-cost edge devices, we further propose smart binarization of our proposed real architecture in subsequent subsections.

#### A. Binary Neural Network

Consider a real valued NN  $g_\phi(\cdot)$ , where  $\phi$  represents the real valued network parameters. The output of the Neural Network is given by  $y = g_\phi(x)$  where  $x$  is the set of input features to the Neural Network. If  $g_\phi(\cdot)$  is a CNN, and lets say that it has  $L$  layers then the parameters of the CNN (filters) are given by  $\phi = \{\mathbf{W}_1, \dots, \mathbf{W}_L\}$  where  $\mathbf{W}_l \in \mathbb{R}^{c_o \times c_i \times k \times k}$  for the  $l^{th}$  layer of a two dimensional CNN. Here  $c_o$  and  $c_i$  represents the input and output channels and  $k$  is the dimension of the filter. The input to the  $l^{th}$  layer are  $\mathbf{a}_l \in \mathbb{R}^{c_i \times h_{in}^w \times h_{in}^h}$  where  $h_{in}^w$  and  $h_{in}^h$  are width and height of the input respectively. The output from  $l^{th}$  layer is  $\mathbf{a}_{l+1} \in \mathbb{R}^{c_o \times h_{out}^w \times h_{out}^h}$ . Here,  $h_{in}^w$ ,  $h_{in}^h$  are spatial dimensions (width and height) of the input and  $h_{out}^w$ ,  $h_{out}^h$  are the spatial dimensions (width and height) of the output respectively. For a BNN, the weights ( $\mathbf{W}$ ) and activations ( $\mathbf{a}$ ) are binarized using the sign function

Layer	Output Volume	Description
input	$1 \times 2 \times 1024$	
conv	$32 \times 2 \times 1024$	$32 \times (3 \times 3)$
		$1 \times \text{BN}$
R-Block A	$32 \times 2 \times 1024$	$2 \times [32 \times (3 \times 3)]$
		$2 \times \text{BN, addition}$
R-Block A	$32 \times 2 \times 1024$	$2 \times [32 \times (3 \times 3)]$
		$2 \times \text{BN, addition}$
R-Block B	$32 \times 1 \times 512$	$2 \times [32 \times (3 \times 3)], [32 \times (1 \times 1)]$
		$3 \times \text{BN, addition}$
R-Block A	$32 \times 1 \times 512$	$2 \times [32 \times (3 \times 3)]$
		$2 \times \text{BN, addition}$
R-Block B	$64 \times 1 \times 256$	$2 \times [64 \times (3 \times 3)], [64 \times (1 \times 1)]$
		$3 \times \text{BN, addition}$
R-Block A	$64 \times 1 \times 256$	$2 \times [64 \times (3 \times 3)]$
		$2 \times \text{BN, addition}$
R-Block B	$128 \times 1 \times 128$	$2 \times [128 \times (3 \times 3)], [128 \times (1 \times 1)]$
		$3 \times \text{BN, addition}$
R-Block A	$128 \times 1 \times 128$	$2 \times [128 \times (3 \times 3)]$
		$2 \times \text{BN, addition}$
pool	$128 \times 1 \times 1$	average-pooling (128)
BN	$128 \times 1 \times 1$	$1 \times \text{BN}$
linear	$24 \times 1 \times 1$	classification into 24 classes
		softmax

TABLE I: Architecture of LResNet18A

before the convolution operation. The binarized parameters corresponding to the  $l^{th}$  layer are given by

$$\mathbf{W}_l^b = \text{sign}(\mathbf{W}_l), \quad \mathbf{a}_l^b = \text{sign}(\mathbf{a}_l). \quad (1)$$

We can further rewrite the convolution operation as convolution performed with the help of bit-wise operations as follows:

$$\mathbf{W}_l * \mathbf{a}_l \approx \mathbf{W}_l^b \circledast \mathbf{a}_l^b \quad (2)$$

where,  $\circledast$  is the convolution operation performed with bit-wise operators. Even though the weights are binarized during the forward pass, to be able to perform back-propagation the Latent weights and real-valued gradients are used. The existence of the sign-function makes it hard to calculate the gradients and hence it is for the same reason that we use a straight-through estimator to pass the gradient during back-propagation. Suppose if  $b = \text{sign}(r)$ , then  $\text{grad}_r = \text{grad}_b \mathbf{1}_{|r| \leq 1}$  where  $\text{grad}_r = \frac{\partial C}{\partial r}$ ,  $\text{grad}_b = \frac{\partial C}{\partial b}$  and  $C$  is the cost function of the NN. The real-valued weights are clipped between  $\{+1, -1\}$  to maintain a stable update. The seminal

work in this area by the authors in [28] was used by us to construct the convolution layers that contain binarized weights and activations. It helped us in changing the setting from Real-Valued to Binary. The binary version of LResnet18A is called *BLResNet18A*. However, simple binarization results in significant degradation of performance though it leads to significant savings in computation and memory. Hence in the next section, we discuss how to circumvent this problem of performance degradation.

### B. Rotated Binary Neural network

In this section, we address one of the major shortcomings of a BNN which is the quantization error that follows due to binarization of the weight vector  $\mathbf{w}_l \in \mathbb{R}^{n_l}$  that belongs to the  $l^{th}$  layer of the Neural Network where  $\mathbf{w}_l$  is the vectorized version of  $\mathbf{W}_l$  and  $n_l = c_o \cdot c_i \cdot k^2$ . The presence of an angular bias between  $\mathbf{w}_l^b$  and  $\mathbf{w}_l$  could lead to a large quantization error and therefore degrade the performance of the network. To reduce the angular bias, at the beginning of each training epoch, very recently [33] proposed an application of a rotation matrix  $\mathbf{R}_l \in \mathbb{R}^{n_l \times n_l}$  to  $\mathbf{w}_l$  such that the angle  $\phi_l$  between  $(\mathbf{R}_l)^T \mathbf{w}_l$  and its binary vector  $\text{sign}((\mathbf{R}_l)^T \mathbf{w}_l)$  is minimized. The equation for the angle is formulated as follows:

$$\cos(\phi_l) = \frac{\text{sign}((\mathbf{R}_l)^T \mathbf{w}_l)^T ((\mathbf{R}_l)^T \mathbf{w}_l)}{\|\text{sign}((\mathbf{R}_l)^T \mathbf{w}_l)\|_2 \|(\mathbf{R}_l)^T \mathbf{w}_l\|_2}, \quad (3)$$

where  $(\mathbf{R}_l)^T \mathbf{R}_l = \mathbf{I}_{n_l}$  is the  $n_l$ -th order identity matrix. Note,  $\|\text{sign}((\mathbf{R}_l)^T \mathbf{w}_l)\|_2 = \sqrt{n_l}$  and  $\|(\mathbf{R}_l)^T \mathbf{w}_l\|_2 = \|\mathbf{w}_l\|_2$ . Since the training happens at the beginning of each epoch, we can take  $\|\mathbf{w}_l\|_2$  to be a constant. Thus Eq. (3) can be simplified as follows:

$$\begin{aligned} \cos(\phi_l) &= \eta_l \cdot \text{sign}((\mathbf{R}_l)^T \mathbf{w}_l)^T ((\mathbf{R}_l)^T \mathbf{w}_l) \\ &= \eta_l \cdot \text{tr}(\mathbf{w}_l^b (\mathbf{w}_l^T \mathbf{R}_l)), \end{aligned} \quad (4)$$

where  $\text{tr}(\cdot)$  is the trace of the input matrix,

$$\begin{aligned} \mathbf{w}_l^b &= \text{sign}((\mathbf{R}_l)^T \mathbf{w}_l), \\ \eta_l &= 1/(\|\text{sign}((\mathbf{R}_l)^T \mathbf{w}_l)\|_2 \|(\mathbf{R}_l)^T \mathbf{w}_l\|_2) \\ &= 1/(\sqrt{n_l} \|\mathbf{w}_l\|_2). \end{aligned} \quad (5)$$

However, Eq. (4) involves a large rotation matrix ( $n_l$  can be large) and hence direct optimization of  $\mathbf{R}_l$  would require massive memory and computation. To reduce that, the authors introduced a scheme using the properties of the Kronecker Product where they split the rotation matrix  $\mathbf{R}_l$  into two smaller rotation matrices  $\mathbf{R}_{l1}$  and  $\mathbf{R}_{l2}$  that gives

$$(\mathbf{w}_l)^T (\mathbf{R}_{l1} \otimes \mathbf{R}_{l2}) = \text{Vec}((\mathbf{R}_{l2})^T (\overline{\mathbf{W}}_l)^T \mathbf{R}_{l1}), \quad (6)$$

where  $\text{Vec}(\cdot)$  vectorizes the input and  $\text{Vec}(\overline{\mathbf{W}}_l) = \mathbf{w}_l$ ,  $\mathbf{R}_{l1} \in \mathbb{R}^{n_{l1} \times n_{l1}}$ ;  $\mathbf{R}_{l2} \in \mathbb{R}^{n_{l2} \times n_{l2}}$ ;  $\overline{\mathbf{W}}_l \in \mathbb{R}^{n_{l2} \times n_{l1}}$ ;  $n_l = n_{l1} n_{l2}$ . Hence, applying a bi-rotation to  $\overline{\mathbf{W}}_l$  is equivalent to applying a  $\mathbf{R}_l = \mathbf{R}_{l1} \otimes \mathbf{R}_{l2}$  where  $\mathbf{R}_l \in \mathbb{R}^{n_{l1} n_{l2} \times n_{l1} n_{l2}}$  rotation to  $\mathbf{w}_l$ . Thus, the authors try to find optimal values for  $\mathbf{R}_{l1}$  and  $\mathbf{R}_{l2}$  which consumes  $\mathcal{O}((n_{l1})^2 + (n_{l2})^2)$  space complexity and  $\mathcal{O}((n_{l1})^2 n_{l2} + (n_{l2})^2 n_{l1})$  time complexity as compared

to  $\mathcal{O}((n_l)^2)$  space and time complexity in the absence of bi-rotation which can make a huge difference. Further, Eq. (4) can be re-written as

$$\begin{aligned} \cos(\phi_l) &= \eta_l \cdot \text{tr}(\mathbf{w}_l^b \text{Vec}((\mathbf{R}_{l2})^T (\overline{\mathbf{W}}_l)^T \mathbf{R}_{l1})) \\ &= \eta_l \cdot \text{tr}(\mathbf{W}_l^b (\mathbf{R}_{l2})^T (\overline{\mathbf{W}}_l)^T \mathbf{R}_{l1}), \end{aligned} \quad (7)$$

where,  $\mathbf{W}_l^b = \text{sign}((\mathbf{R}_{l1})^T \overline{\mathbf{W}}_l \mathbf{R}_{l2})$ ,  
 $(\mathbf{R}_{l1})^T \mathbf{R}_{l1} = \mathbf{I}_{n_{l1}}$   
 $(\mathbf{R}_{l2})^T \mathbf{R}_{l2} = \mathbf{I}_{n_{l2}}$ .

Hence, the optimization objective is given by:

$$\begin{aligned} \arg \max_{\mathbf{W}_l^b, \mathbf{R}_{l1}, \mathbf{R}_{l2}} \quad & \text{tr}(\mathbf{W}_l^b (\mathbf{R}_{l2})^T (\overline{\mathbf{W}}_l)^T \mathbf{R}_{l1}) \\ \text{s.t. } \quad & \mathbf{W}_l^b \in \{+1, -1\}^{n_{l1} \times n_{l2}} \\ & (\mathbf{R}_{l1})^T \mathbf{R}_{l1} = \mathbf{I}_{n_{l1}} \\ & (\mathbf{R}_{l2})^T \mathbf{R}_{l2} = \mathbf{I}_{n_{l2}}. \end{aligned} \quad (8)$$

Since the above optimization is not a convex problem, the authors proposed an alternating optimization approach, where one variable is updated keeping the rest two fixed until convergence. We, therefore, have three steps of optimization given by:

- 1) The first step is to learn  $\mathbf{W}_l^b$  while fixing  $\mathbf{R}_{l1}$  and  $\mathbf{R}_{l2}$ . Therefore the optimization reduces to

$$\begin{aligned} \arg \max_{\mathbf{W}_l^b} \quad & \text{tr}(\mathbf{W}_l^b (\mathbf{R}_{l2})^T (\overline{\mathbf{W}}_l)^T \mathbf{R}_{l1}) \\ \text{s.t. } \quad & \mathbf{W}_l^b \in \{+1, -1\}^{n_{l1} \times n_{l2}} \\ & (\mathbf{R}_{l1})^T \mathbf{R}_{l1} = \mathbf{I}_{n_{l1}} \\ & (\mathbf{R}_{l2})^T \mathbf{R}_{l2} = \mathbf{I}_{n_{l2}} \end{aligned} \quad (9)$$

which is solved by  $\mathbf{W}_l^b = \text{sign}((\mathbf{R}_{l1})^T \overline{\mathbf{W}}_l \mathbf{R}_{l2})$ .

- 2) This step updates  $\mathbf{R}_{l1}$  while keeping  $\mathbf{W}_l^b$  and  $\mathbf{R}_{l2}$  constant. The corresponding sub-problem is

$$\begin{aligned} \arg \max_{\mathbf{R}_{l1}} \quad & \text{tr}(\mathbf{G}_{l1} \mathbf{R}_{l1}) \\ \text{s.t. } \quad & (\mathbf{R}_{l1})^T \mathbf{R}_{l1} = \mathbf{I}_{n_{l1}}, \end{aligned} \quad (10)$$

where  $\mathbf{G}_{l1} = \mathbf{W}_l^b (\mathbf{R}_{l2})^T (\overline{\mathbf{W}}_l)^T$ . In order to find the optimal  $\mathbf{R}_{l1}$ ,  $\mathbf{G}_{l1}$  is polar decomposed using SVD as

$$\mathbf{G}_{l1} = \mathbf{U}_{l1} \mathbf{S}_{l1} (\mathbf{V}_{l1})^T \quad (11)$$

that yields

$$\mathbf{R}_{l1} = \mathbf{V}_{l1} (\mathbf{U}_{l1})^T. \quad (12)$$

- 3) Similar to the previous steps, the following step updates  $\mathbf{R}_{l2}$  while keeping  $\mathbf{W}_l^b$  and  $\mathbf{R}_{l1}$  constant. The corresponding sub-problem is

$$\begin{aligned} \arg \max_{\mathbf{R}_{l2}} \quad & \text{tr}((\mathbf{R}_{l2})^T \mathbf{G}_{l2}) \\ \text{s.t. } \quad & (\mathbf{R}_{l2})^T \mathbf{R}_{l2} = \mathbf{I}_{n_{l2}} \end{aligned}, \quad (13)$$

where  $\mathbf{G}_{l2} = (\overline{\mathbf{W}}_l)^T \mathbf{R}_{l1} \mathbf{W}_l^b$ . To find the optimal  $\mathbf{R}_{l2}$ ,  $\mathbf{G}_{l2}$  is polar decomposed using SVD as

$$\mathbf{G}_{l2} = \mathbf{U}_{l2} \mathbf{S}_{l2} (\mathbf{V}_{l2})^T \quad (14)$$

that yields

$$\mathbf{R}_{l2} = \mathbf{U}_{l2}(\mathbf{V}_{l2})^T. \quad (15)$$

The above mentioned optimization steps are performed iteratively for maximum of three cycles until  $\mathbf{W}'_{l1}$ ,  $\mathbf{R}_{l1}$ , and  $\mathbf{R}_{l2}$  are converged. However, the above optimization could get caught in a local optimum. Hence, the authors further propose the adjustable rotated weight vector scheme in order to reduce the angular bias after the bi-rotation step. Instead of using the rotated weights as they are,

$$\tilde{\mathbf{w}}_l = (\mathbf{R}_l)^T \mathbf{w}_l \quad (16)$$

they propose the usage of the following update equation

$$\tilde{\mathbf{w}}_l = \mathbf{w}_l + ((\mathbf{R}_l)^T \mathbf{w}_l - \mathbf{w}_l) \cdot \alpha_l, \quad (17)$$

where,  $\alpha_l = |\sin(\beta_l)| \in [0, 1]$  and  $\beta_l \in \mathbb{R}$ .

During training the RBLResNet18A, at the beginning of every training epoch, the rotation matrices,  $\mathbf{R}_{l1}$  and  $\mathbf{R}_{l2}$  are learned for fixed parameters  $\mathbf{w}_l$ . At the training phase, with the fixed  $\mathbf{R}_{l1}$  and  $\mathbf{R}_{l2}$ , the neural network takes the sign of parameter  $\tilde{\mathbf{w}}_l$  for the forward pass and the parameters  $\mathbf{w}_l$  and  $\beta_l$  are updated during back-propagation.

While constructing RBLResNet18A, we apply RBNN on the parameters of all the convolutional layers except the one that is next to the input and output. The first convolution layer is left to be a real layer to extract features from the input more efficiently and the last linear layer is also real. The number of FLOPs and memory required for the same have been reported in Table. II. We emphasize that if we apply RBNN or BNN blindly to existing architectures, the performance degradation is huge. However, applying the RBNN concept to our proposed architecture only leads to a 10% degradation when compared to the real variant while the memory and computation savings are huge. In the next subsection, we try to close the gap further.

### C. Ensemble of RBNN

In [27] the authors have shown that an ensemble of weak BNNs can perform as well as real-valued networks. Inspired by this, in the context of TurboAEs we propose an ensemble of multiple RBLResNet18A using bagging [36] to get *RBLResNet18A-Bag* and hence achieve better accuracy. In machine learning, bagging is known to improve stability, accuracy and to reduce variance. We ensemble  $B$  such RBLResNet18As to get *RBLResNet18A-Bag*. In bagging method, the linear layer output from each one of these  $B$  RBLResNet18As ( $\hat{u}^1, \dots, \hat{u}^B$ ) are averaged to get the final output  $\hat{u} = \frac{1}{B} \sum_{b=1}^B \hat{u}^b$  that is passed via softmax and used for classification. We have taken ensemble of two and four RBLResNet18As and called them *RBLResNet18A-Bag2* and *RBLResNet18A-Bag4* respectively.

### D. Savings in Computation

The total number of FLOPs combining multiplication and addition for the  $l$ th layer is  $2 \times c_i \times k^2 \times h_{out}^w \times h_{out}^h \times c_o$ . The main motivation of the proposed system is to save on computational complexity and memory. We achieve that by

using BNNs and RBNNs with better performance using the latter. BNN and RBNN convert weights and activations into binary  $\{+1, -1\}$ , therefore making it possible to carry out convolution operations using the efficient xnor and bitcount logic instead of Floating Point (FLOP) operations. Hence in Table. II for all the binary parameters in BNN or RBNN, the FLOPs are replaced by XNOR counts. Whereas a single FLOP count operation needs one 64 bit register for 64 bit floating point operation, using the same 64 bit register, 64 single bit xnor-count operations can be computed which makes the system almost 64 times faster than the real networks. For a 64 bit system, the same number of real-valued parameters take 64 times more memory than binary parameters in BNNs and RBNNs. These advantages make the system a perfect fit for use in edge devices that are typically limited in memory and power. Ensemble of  $B$  such networks (BNNs and RBNNs) improve on accuracy but has  $B$  times the memory requirements. The computational complexity is however same as a single BNN or RBNN by the use of parallel processing of  $B$  such networks.

## IV. EXPERIMENTS

The industry-standard data set, and its following updates, for modulation classification in radio is given by [14], [37]. In [20] they had released an updated version of the dataset named the RML2018.01a (R: Radio; ML: Machine Learning) dataset. It is composed of 24 modulations schemes namely OOK, 4ASK, 8ASK, BPSK, QPSK, 8PSK, 16PSK, 32PSK, 16APSK, 32APSK, 64APSK, 128APSK, 16QAM, 32QAM, 64QAM, 128QAM, 256QAM, AM-SSB-WC, AM-SSB-SC, AM-DSB-WC, AM-DSB-SC, FM, GMSK, OQPSK, with 26 evenly spaced bins in signal-to-noise ratio (SNR), ranging from  $-20$  to  $30$  dB. The set is composed of 2,555,904 I/Q (in-phase/quadrature) signals each of length 1024. The dataset contains both synthetic simulated channel effects and over-the-air recordings. The synthetic data were produced using software defined radio programmed with GNU radio [38]. This particular version of the dataset is stored in the hdf5 format and hence the appropriate libraries were used to extract the data.

All the experiments were performed using a system equipped with 3.00 GHz CPU, 64 GB RAM, and an NVIDIA Geforce RTX 2080Ti GPU. As model training options, RBNN is end-to-end trained with random initial weights in 200 epochs using the stochastic gradient descent optimizer with the momentum of 0.9. The mini-batch size for each iteration is set to 256 and the learning rate is initialized at 0.01. The experiments use the cosine-annealing learning rate scheduler, where the learning rate is often restarted to simulate a warm restart. Out of the complete dataset, 75% of the samples are used for training, and the rest for testing. We use the categorical cross-entropy loss function where the number of classes can be changed according to the RML Dataset being used. We have compared the proposed architecture in different settings with SOTA architectures in terms of performance and efficiency. In the case of MCNet and RMLResNet, we simulate them with the RBNN setting as well and add them in the comparison.

Setting	Model	Computation	Parameters	Memory Req (MB)	Accuracy % at 10dB
Real valued	RMLResNet	$\approx 1.3e8$ FLOPs	2.37e5	1.9	91.47
	MCNet ( $m = 10$ )	$\approx 1.9e7$ FLOPs	2.20e5	1.76	92.25
	InvoResNet	$\approx 1.7e10$ FLOPs	2.20e5	1.76	95
	LightWeight	$\approx 8.9e7$ FLOPs	5.00e4	0.4	91.48
	<b>LResNet18A</b>	$\approx 4.5e8$ FLOPs	7.36e5	<b>5.8</b>	<b>95.76</b>
BNN	BLResNet18A	$\approx 4.5e8$ XNOR counts	7.36e5	0.09	35
BNN with 2 real layers	BLResNet18A2real	$\approx 4.5e8$ XNOR counts + $1.1e6$ FLOPs	7.36e5	0.12	57.47
RBNN	RMLResNet	$\approx 1.2e8$ XNOR counts + $1.0e6$ FLOPs	2.37e5	0.7	59.533
	MCNet ( $m = 10$ )	$\approx 1.7e7$ XNOR counts + $2.5e6$ FLOPs	2.20e5	0.11	62.2
	<b>RBLResNet18A</b>	$\approx 4.5e8$ XNOR counts + $1.1e6$ FLOPs	7.36e5	<b>0.12</b>	<b>85.33</b>
	<b>RBLResNet18A-Bag2</b>	$\approx 4.5e8$ XNOR counts + $1.1e6$ FLOPs	1.47e6	<b>0.24</b>	<b>86.72</b>
	<b>RBLResNet18A-Bag4</b>	$\approx 4.5e8$ XNOR counts + $1.1e6$ FLOPs	2.94e6	<b>0.48</b>	<b>87.74</b>

TABLE II: Savings vs performances of different networks on the RML2018.01a dataset. Note, a total of 64 XNOR count operations is equivalent to 1 FLOP using a 64 bit register.

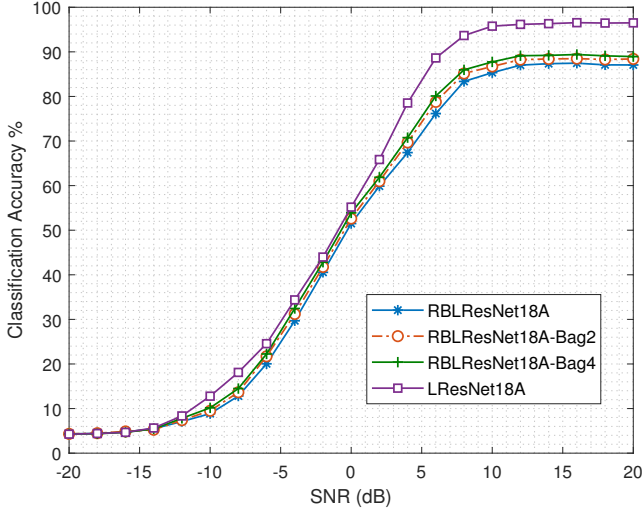


Fig. 2: Improvement in accuracy by taking ensemble

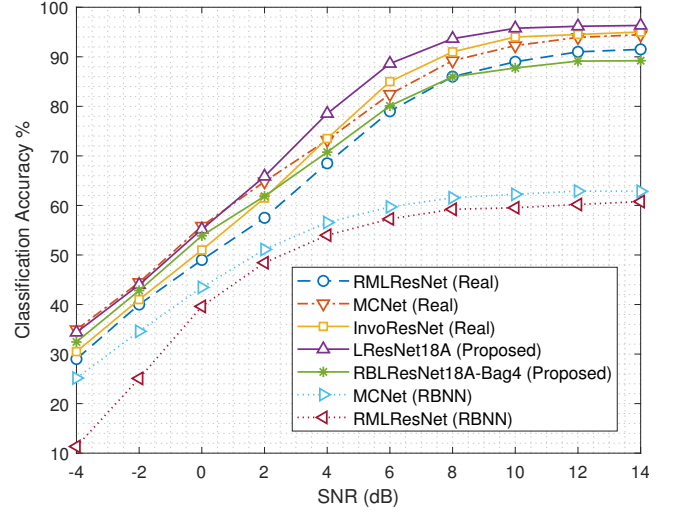


Fig. 3: Accuracy vs SNR for different architectures

### A. Results

On RML2018.01a, the proposed RBLResNet18A and its ensemble versions are compared with several SOTA architectures like MCNet and RMLResNet. We list the experimental results in Table II. As can be seen, the proposed real-valued LResNet18A architecture outperforms the SOTA architectures with 95.76% accuracy, whereas MCNet with 10 M-blocks and RMLResNet have 92.25% and 91.47% accuracy respectively at 10dB SNR. However, because of parameters, the real-valued proposed architecture requires a high memory of 5.8MB and 3.46 times and 23.68 times more computation than RMLResNet and MCNet respectively. The deployment of LResNet18A is suitable when the devices have enough memory and computing resources. The recently proposed InvoResNet has 95% accuracy and comes at the cost of 2090 times more computational complexity than the proposed real architecture. Therefore after binarization, the computation cost cannot be comparable to the BNN/RBNN version of the proposed architecture thus it is not considered for comparison. The proposed architecture has a better overall accuracy<sup>1</sup> of 61.65% than other SOTA architectures (for instance, MCNet

has an overall accuracy of 60.4%). Although the binarized version BLResNet18A was able to classify with an overall accuracy of 23.66%, the binarized version of MCNet and the RMLResNet architectures failed to learn any meaningful features and were performing close to random, thus not included in the table. It implies that binarizing any real network blindly may not preserve accuracy. It is supported by [19] which shows that just binarizing LSTM or traditional CNN does not give good results when used for AMC. We also take an architecture named *BLResnet18A2real* where the layers next to the input and output layers are taken as real to have more information passing from the input layer to the network similar to RBNN architecture. It is observed that it improves the performance with 39.40% overall accuracy.

The RBNN version of the proposed architecture achieves an accuracy of 85.33% with a significant improvement of 23.13% and 25.797% over the RBNN version of MCNet and RMLResNet at 10dB SNR, at the same time saving on memory and computational complexity. The RBLResNet18A has a memory requirement of 0.12 MB which is lower than any other real network. For the RBNN version of MCNet, even though it has a comparable memory requirement of 0.106 MB and comparable computational com-

<sup>1</sup>by overall accuracy we mean the accuracy averaged over all SNRs



plexity, it has a way lower accuracy of 62.2% at 10dB and almost random classification on an average. Similarly, RMLResNet's RBNN version has poor accuracy with 7 times more memory requirement. The LightWeight architecture has 3.3 times more memory requirement and 11 times more computational complexity than RBLResNet18A. The overall accuracy for proposed RBLResNet18A, RBLResNet18A-Bag2, RBLResNet18A-Bag4 are higher (55.11%, 56.21%, 56.88% respectively) whereas the RBNN version of MCNet and RMLResNet are comparatively lower (41.47% and 38.29% respectively). The performance of ensemble networks is shown in Fig. 2. The ensemble version of the proposed system has an improvement of 1.4% and 2.4% at 10dB for the ensemble of  $B = 2$  and  $B = 4$  networks respectively without compromising much on memory requirements with 0.24 MB and 0.48 MB respectively. An accuracy versus SNR plot for the architectures is shown in Fig. 3. For all the SNRs, the proposed LResNet18A performs equally well or better than InvoResNet. The proposed RBLResNet18A-Bag4 also performs close to real-valued RMLResNet and MCNet.

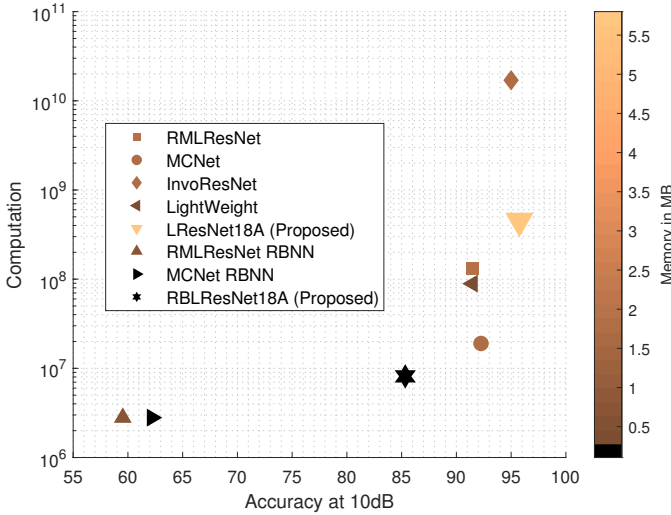


Fig. 4: Memory vs Computation vs Accuracy at 10dB

In Fig. 4 we have compared memory, computation, and the accuracy of all the architectures. The methods that lie in the bottom right part of the scatter plot have maximum accuracy and need the least computing power. The memory requirement is shown by the color map. It clearly shows that the proposed binarized version has the lowest computation and memory requirement out of all without compromising much on accuracy.

## V. CONCLUSION

In summary, we first propose a DL architecture which outperforms existing DL methods. Next we propose RBLResNet18A in order to deploy Automatic Modulation Classification with a large number of classes on targeted low power edge devices by reducing the memory requirement and the computations by nearly 64 times at the cost of acceptable performance degradation over real networks. We then propose RBLResNet18A-Bag to improve the performance offered by

a single RBLResNet18A and achieve performance close to the real networks. The ensemble technique implemented with four such weak learners is shown to consume 48 times less memory and 64 times lesser computational requirement than the real-valued SOTA architectures with the nearly similar performance which makes them an excellent fit for such edge devices.

## REFERENCES

- [1] V. Gouldieff, J. Palicot, and S. Daumont, "Blind modulation classification for cognitive satellite in the spectral coexistence context," *IEEE Transactions on Signal Processing*, vol. 65, no. 12, pp. 3204–3217, 2017.
- [2] L. M. Hoang, M. Kim, and S.-H. Kong, "Automatic recognition of general lpi radar waveform using ssd and supplementary classifier," *IEEE Transactions on Signal Processing*, vol. 67, no. 13, pp. 3516–3530, 2019.
- [3] B. Kim, J. Kim, H. Chae, D. Yoon, and J. W. Choi, "Deep neural network-based automatic modulation classification technique," in *2016 International Conference on Information and Communication Technology Convergence (ICTC)*. IEEE, 2016, pp. 579–582.
- [4] L. Häring, Y. Chen, and A. Czylik, "Automatic modulation classification methods for wireless ofdm systems in tdd mode," *IEEE transactions on communications*, vol. 58, no. 9, pp. 2480–2485, 2010.
- [5] Y. Shi and X.-D. Zhang, "A gabor atom network for signal classification with application in radar target recognition," *IEEE Transactions on signal processing*, vol. 49, no. 12, pp. 2994–3004, 2001.
- [6] C.-Y. Huan and A. Polydoros, "Likelihood methods for mpsk modulation classification," *IEEE Transactions on Communications*, vol. 43, no. 2/3/4, pp. 1493–1504, 1995.
- [7] W. Wei and J. M. Mendel, "Maximum-likelihood classification for digital amplitude-phase modulations," *IEEE transactions on Communications*, vol. 48, no. 2, pp. 189–193, 2000.
- [8] A. Ramezani-Kebrya, I.-M. Kim, D. I. Kim, F. Chan, and R. Inkol, "Likelihood-based modulation classification for multiple-antenna receiver," *IEEE Transactions on Communications*, vol. 61, no. 9, pp. 3816–3829, 2013.
- [9] A. Swami and B. M. Sadler, "Hierarchical digital modulation classification using cumulants," *IEEE Transactions on communications*, vol. 48, no. 3, pp. 416–429, 2000.
- [10] S. S. Soliman and S.-Z. Hsue, "Signal classification using statistical moments," *IEEE Transactions on Communications*, vol. 40, no. 5, pp. 908–916, 1992.
- [11] Q. Shi and Y. Karasawa, "Automatic modulation identification based on the probability density function of signal phase," *IEEE Transactions on Communications*, vol. 60, no. 4, pp. 1033–1044, 2012.
- [12] Y. A. Eldemerdash, M. Marey, O. A. Dobre, G. K. Karagiannidis, and R. Inkol, "Fourth-order statistics for blind classification of spatial multiplexing and alamouti space-time block code signals," *IEEE Transactions on Communications*, vol. 61, no. 6, pp. 2420–2431, 2013.
- [13] F. Meng, P. Chen, L. Wu, and X. Wang, "Automatic modulation classification: A deep learning enabled approach," *IEEE Transactions on Vehicular Technology*, vol. 67, no. 11, pp. 10760–10772, 2018.
- [14] T. J. O'Shea, J. Corgan, and T. C. Clancy, "Convolutional radio modulation recognition networks," in *International conference on engineering applications of neural networks*. Springer, 2016, pp. 213–226.
- [15] S. Huang, Y. Jiang, Y. Gao, Z. Feng, and P. Zhang, "Automatic modulation classification using contrastive fully convolutional network," *IEEE Wireless Communications Letters*, vol. 8, no. 4, pp. 1044–1047, 2019.
- [16] A. P. Hermawan, R. R. Ginanjar, D.-S. Kim, and J.-M. Lee, "Cnn-based automatic modulation classification for beyond 5g communications," *IEEE Communications Letters*, vol. 24, no. 5, pp. 1038–1041, 2020.
- [17] S. Peng, H. Jiang, H. Wang, H. Alwageed, Y. Zhou, M. M. Sebdani, and Y.-D. Yao, "Modulation classification based on signal constellation diagrams and deep learning," *IEEE transactions on neural networks and learning systems*, vol. 30, no. 3, pp. 718–727, 2018.
- [18] G. J. Mendis, J. Wei, and A. Madanayake, "Deep belief network for automated modulation classification in cognitive radio," in *2017 Cognitive Communications for Aerospace Applications Workshop (CCAA)*. IEEE, 2017, pp. 1–5.
- [19] S. Rajendran, W. Meert, D. Giustiniano, V. Lenders, and S. Pollin, "Deep learning models for wireless signal classification with distributed low-cost spectrum sensors," *IEEE Transactions on Cognitive Communications and Networking*, vol. 4, no. 3, pp. 433–445, 2018.

- [20] T. J. O'Shea, T. Roy, and T. C. Clancy, "Over-the-air deep learning based radio signal classification," *IEEE Journal of Selected Topics in Signal Processing*, vol. 12, no. 1, pp. 168–179, 2018.
- [21] S. Huang, L. Chai, Z. Li, D. Zhang, Y. Yao, Y. Zhang, and Z. Feng, "Automatic modulation classification using compressive convolutional neural network," *IEEE Access*, vol. 7, pp. 79 636–79 643, 2019.
- [22] K. He, X. Zhang, S. Ren, and J. Sun, "Deep residual learning for image recognition," in *Proceedings of the IEEE conference on computer vision and pattern recognition*, 2016, pp. 770–778.
- [23] F. Wang and X. Wang, "Fast and robust modulation classification via kolmogorov-smirnov test," *IEEE Transactions on Communications*, vol. 58, no. 8, pp. 2324–2332, 2010.
- [24] S.-H. Kim, J.-W. Kim, V.-S. Doan, and D.-S. Kim, "Lightweight deep learning model for automatic modulation classification in cognitive radio networks," *IEEE Access*, vol. 8, pp. 197 532–197 541, 2020.
- [25] H. Zhang, L. Yuan, G. Wu, F. Zhou, and Q. Wu, "Automatic modulation classification using involution enabled residual networks," *IEEE Wireless Communications Letters*, 2021.
- [26] Y. Wang, L. Guo, Y. Zhao, J. Yang, B. Adebisi, H. Gacanin, and G. Gui, "Distributed learning for automatic modulation classification in edge devices," *IEEE Wireless Communications Letters*, vol. 9, no. 12, pp. 2177–2181, 2020.
- [27] D. Vikas, N. Nayak, and S. Kalyani, "Realizing neural decoder at the edge with ensembled bnn," *IEEE Communications Letters*, pp. 1–1, 2021.
- [28] I. Hubara, M. Courbariaux, D. Soudry, R. El-Yaniv, and Y. Bengio, "Binarized neural networks," *Advances in neural information processing systems*, vol. 29, 2016.
- [29] M. Rastegari, V. Ordonez, J. Redmon, and A. Farhadi, "Xnor-net: Imagenet classification using binary convolutional neural networks," in *European conference on computer vision*. Springer, 2016, pp. 525–542.
- [30] X. He, Z. Mo, K. Cheng, W. Xu, Q. Hu, P. Wang, Q. Liu, and J. Cheng, "Proxybnn: Learning binarized neural networks via proxy matrices," in *Computer Vision–ECCV 2020: 16th European Conference, Glasgow, UK, August 23–28, 2020, Proceedings, Part III 16*. Springer, 2020, pp. 223–241.
- [31] J. Song, Y. Wang, M. Guo, X. Ji, K. Cheng, Y. Hu, X. Tang, R. Wang, and R. Huang, "Td-sram: Time-domain-based in-memory computing macro for binary neural networks," *IEEE Transactions on Circuits and Systems I: Regular Papers*, 2021.
- [32] I. Hubara, M. Courbariaux, D. Soudry, R. El-Yaniv, and Y. Bengio, "Quantized neural networks: Training neural networks with low precision weights and activations," *The Journal of Machine Learning Research*, vol. 18, no. 1, pp. 6869–6898, 2017.
- [33] M. Lin, R. Ji, Z. Xu, B. Zhang, Y. Wang, Y. Wu, F. Huang, and C.-W. Lin, "Rotated binary neural network," *Advances in Neural Information Processing Systems*, vol. 33, 2020.
- [34] T. Huynh-The, C.-H. Hua, Q.-V. Pham, and D.-S. Kim, "Mcnet: An efficient cnn architecture for robust automatic modulation classification," *IEEE Communications Letters*, vol. 24, no. 4, pp. 811–815, 2020.
- [35] T. Courtat and H. d. M. d. Bourboux, "A light neural network for modulation detection under impairments," *arXiv preprint arXiv:2003.12260*, 2020.
- [36] S. Zhu, X. Dong, and H. Su, "Binary ensemble neural network: More bits per network or more networks per bit?" in *Proceedings of the IEEE/CVF Conference on Computer Vision and Pattern Recognition*, 2019, pp. 4923–4932.
- [37] T. J. O'Shea, J. Corgan, and T. C. Clancy, "Unsupervised representation learning of structured radio communication signals," in *2016 First International Workshop on Sensing, Processing and Learning for Intelligent Machines (SPLINE)*. IEEE, 2016, pp. 1–5.
- [38] E. Blossom, "Gnu radio: Tools for exploring the radio frequency spectrum," *Linux J.*, vol. 2004, no. 122, p. 4, Jun. 2004.